Prediction of gas/particle partitioning of polybrominated diphenyl ethers (PBDEs) in global air: A theoretical study

Yi-Fan Li[1,2,3], Wan-Li Ma[1], Meng Yang[2]

[1] International Joint Research Center for Persistent Toxic Substances (IJRC-PTS), State Key Laboratory of Urban Water Resource and Environment/School of Municipal and Environmental Engineering, Harbin Institute of Technology, Harbin 150090, P. R. China

[2] IJRC-PTS, Dalian Maritime University, Dalian, 116026, P. R. China

[3] IJRC-PTS-NA, Toronto, Ontario, M2N 6X9, Canada

Correspondence and requests for materials should be addressed to YFL (email: ijrc_pts_paper@yahoo.com)

Abstract

Gas/particle (G/P) partitioning for semivolatile organic compounds (SVOCs) is an important process that primarily governs their atmospheric fate, long-range atmospheric transport, and their routes to enter human body. All previous studies on this issue have hypothetically based on equilibrium condition, the results of which do not predict results from monitoring studies well in most cases. In this study, a *steady-state* model instead of an equilibrium-state model for the investigation of the G/P partitioning behavior for polybrominated diphenyl ethers (PBDEs) was established, and an equation for calculating the partition coefficients under *steady state* (K_{PS}) for PBDE congeners ($\log K_{PS} = \log K_{PE} + \log\alpha$) was developed, in which an equilibrium term ($\log K_{PE} = \log K_{OA} + \log f_{OM} - 11.91$, where f_{OM} is organic matter content of the particles) and a nonequilibrium term ($\log\alpha$, caused by dry and wet depositions of particles), both being functions of $\log K_{OA}$ (octanol-air partition coefficient), are included. It was found that the equilibrium is a special case of *steady state* when the nonequilibrium term equals to zero. A criterion to classify the equilibrium and nonequilibrium status for PBDEs was also established using two threshold values of $\log K_{OA}$, $\log K_{OA1}$ and $\log K_{OA2}$, which divide the range of $\log K_{OA}$ into 3 domains: equilibrium, nonequilibrium, and maximum partition domain; and accordingly, two threshold values of temperature t, t_{TH1} when $\log K_{OA} = \log K_{OA1}$ and t_{TH2} when $\log K_{OA} = \log K_{OA2}$, were identified, which divide the range of temperature also into the same 3 domains for each PBDE congener. We predicted the existence of the maximum partition domain (the values of $\log K_{PS}$ reach a maximum constant of -1.53) that every PBDE congener can reach when $\log K_{OA} \geq \log K_{OA2}$, or $t \leq t_{TH2}$. The novel equation developed in this study was applied to predict the G/P partition coefficients of PBDEs for the published monitoring data worldwide, including Asia, Europe, North America, and the Arctic, and the results matched well with all the monitoring data, except those obtained at e-waste sites due to the unpredictable PBDE emissions at these sites.

This study provided evidence that, the newly developed *steady-state*-based equation is superior to the equilibrium-state-based equation that has been used in describing the G/P partitioning behavior in decades. We suggest that, the investigation on G/P partitioning behavior for PBDEs should be based on *steady state*, not equilibrium state, and equilibrium is just a special case of *steady state* when nonequilibrium factors can be ignored. We also believe that our new equation provides a useful tool for environmental scientists in both monitoring and modeling research on G/P partitioning for PBDEs and can be extended to predict G/P partitioning behavior for other SVOCs as well.

1 Introduction

Atmospheric transport is a major mechanism to move semivolatile organic compounds (SVOCs), including persistent organic pollutants (POPs), from source regions to other remote places, including Arctic and Antarctic, where these chemicals have never been produced and used (Barrie et al. 1992; Macdonald et al. 2000; Li et al.1998; Li and Bidleman, 2003; Eckhardt and Manø, 2007). The gas/particle (also called aerosol) (G/P) partitioning for SVOCs is a very important process that primarily governs their atmospheric fate (Lohmann et al., 2000), since wet and dry depositions and other processes act differently on gaseous and particulate SVOCs, thus affecting the efficiency and scope of their long-range atmospheric transport and fate (Bidleman, 1988). In addition, SVOCs are an important class of indoor pollutants that are of great health concern to humans (Weschler and Nazaroff, 2008). The gaseous and particulate SVOCs have different routes to enter human body, and therefore the G/P partitioning for SVOCs has a significant influence on human exposure (Weschler, 2003).

The G/P partitioning behavior of SVOCs, K_P, is commonly defined as (Yamasaki et al. 1982, Pankow 1991, Pankow and Bidleman 1991)

$$K_P = (C_P/TSP)/C_G \qquad (1)$$

where C_G and C_P are concentrations of SVOCs in gas- and particle-phases (both in pg m^{-3} of air), respectively, and TSP is the concentration of total suspended particle in air (μg m^{-3}). Thus K_P has a unit of m^3 μg^{-1}. In this study, the term of *partition quotient* instead of *partition coefficient*, is used for K_P, because *partition coefficient* is used for equilibrium condition only, and Eq. (1) was not defined under equilibrium condition.

The value of K_P, calculated by Eq. (1) using the monitoring data TSP, C_P, and C_G, is denoted as K_{PM} (subscript "M" in K_{PM} means measurement). It has been shown that there is a linear relationship between $\log K_{PM}$ and $\log K_{OA}$ (K_{OA} is octanol-air partition coefficient)

(Finizio et al. 1997, Harner and Bidleman, 1998, Pankow, 1998) and between logK_{PM} and logP_L (P_L is sub-cooled liquid vapor pressure) (Pankow, 1987; Bidleman and Foreman, 1987; Pankow and Bidleman, 1991, 1992). The logK_{OA}-based model given by

$$\log K_{PR} = m_O \log K_{OA} + b_O \quad (2)$$

has been widely used in describing the partitioning behavior for SVOCs, where slope m_O and intercept b_O are fitting constants obtained using regression of logK_{PM} (from Eq. (1)) against logK_{OA}. The subscript "R" in K_{PR} indicates regression.

Unfortunately, Eq. (2) is not very useful to environmental modelers, since this equation can only be used when the monitoring data of SVOCs concentrations in both gas- and particle-phases are known, while the modelers need the equations to predict environmental behavior, including their concentrations in air with both gas- and particle-phases, based on physicochemical properties of SVOCs, their emissions, climate and meteorological conditions.

Under the conditions of the equilibrium (m_O=1), the dominant absorption processes between gas- and particle-phases, and equivalence of octanol to the sorbing organic matter in particle, Harner and Bidleman (1998) derived the following equation,

$$\log K_{PE} = \log K_{OA} + \log f_{OM} - 11.91 \quad (3)$$

where f_{OM} is organic matter content of the particle. The subscript "E" in K_{PE} indicates equilibrium. In comparison to Eq. (2), Eq. (3) has an advantage to predict K_{PE} from the values of K_{OA} and f_{OM} without the need of real monitoring data.

However, as discussed in the previous publications (Finizio et al., 1997; Cetin and Odabasi, 2007; Tian et al., 2011; Yang et al., 2013; Li and Jia, 2014), Eq. (3) cannot describe accurately the relationship between gas- and particle-phases polybrominated diphenyl ethers (PBDEs). It is evident that Eq. (3) can be applied only in a few cases, such as for less brominated PBDE congeners (such as BDE-17 and -28) or at high temperatures, and becomes inaccurate in most cases, especially for highly brominated PBDE congeners, such as BDE-66, -85, -99, -100, -153, -154, and -183, or at low temperatures (Yang et al., 2013; Li and Jia, 2014). This has been blamed by the artifacts and nonequilibrium factors (Finizio et al., 1997; Cetin and Odabasi, 2007; Tian et al., 2011; Su et al., 2006).

Based on a large dataset of more than 700 pairs of air samples in both gas- and particle-phases with a wide ambient temperature range of 60 ^{o}C from -22 to +38 ^{o}C obtained from our Chinese POPs Soil and Air Monitoring Program, Phase 2 (China-SAMP-II), we investigated G/P partitioning behavior of PBDEs in Chinese air (Yang et al., 2013; Li and Jia, 2014). We derived for the first time empirical equations to predict the values of slopes and intercepts for both K_{OA}-based and P_L-based models as functions of temperature, and thus predicted partition quotient (K_P) without assuming an equilibrium status and free of artifacts (Li and Jia, 2014). The slope m_O and the intercept b_O were given as functions of temperature (in ^{o}C),

$$m_O(t) = 0.011t + 0.263 \tag{4}$$

$$b_O(t) = -(0.135t + 5.006) \tag{5}$$

The temperature t in Eqs. (4) and (5) is usually a mean value of temperature for a series of sampling events, such as annual or monthly mean temperature at each sampling site. After the values of m_O and b_O are calculated using Eqs. (4) and (5), we can use Eq. (2) to calculate the values of logK_P. Since this method can be used to predict the values of logK_P, we use K_{PP} (the second "P" in the subscript K_{PP} indicates "Prediction") instead of K_{PR} in Eq. (2), and rewrite them as

$$\log K_{PP} = m_O(t) \log K_{OA} + b_O(t) \tag{6}$$

where $m_O(t)$ and $b_O(t)$ are given by Eqs. (4) and (5), respectively.

It is noteworthy that logK_{PP} in Eq. (6) depends on two parameters, temperature t and K_{OA}, which is also a function of temperature, and given by an empirical equation (Harner and

Shoeib, 2002)

$$\log K_{OA} = A+B/(t+273.15) \quad (7)$$

where t (in ^{o}C) is the temperature for each sampling event, and the parameters A and B are given in **Table S1** in the Supplement for several PBDE congeners. It should be borne in mind that temperature t in Eqs. (4) and (5) can be also the temperature for each sampling event, and thus using Eq. (7), we can express $\log K_{PP}$ in Equation (6) as a function of a single independent variable of $\log K_{OA}$ as (Li and Jia, 2014)

$$\log K_{PP}\ (K_{OA})=0.011B(\log K_{OA}–12.27)/(\log K_{OA}–A)–2.74\log K_{OA}+31.85 \quad (8)$$

These two Eqs. (6) and (8) have been successfully applied to predict the values of K_P for PBDEs as functions of $\log K_{OA}$ in air of China and other countries in the north temperate zone and also at an Arctic site in East Greenland (Li and Jia, 2014), and our results matched the monitoring data well at background, rural, urban, and suburban sites, but not at e-waste sites due to the unpredictable PBDE emissions at these sites, and the results indicated that our new equations have a better performance than Eq. (3) in describing G/P partitioning behavior of PBDEs in air as functions of $\log K_{OA}$. We also found for the first time that the G/P partitioning of PBDE congeners can reach a maximum value if the ambient temperature is low enough. A criterion to classify the equilibrium and nonequilibrium status for PBDEs was also established using $\log K_{OA}$ (Li and Jia, 2014).

These equations, however, suffer from two drawbacks. First, these equations derived at the temperature range from -22 to +38 ^{o}C, thus cannot be used at temperatures beyond this range; secondly, these equations were obtained empirically, and do not have a strong theoretical foundation. Therefore, in this paper, we study the G/P partitioning behavior of PBDEs in global air in a theoretical way. The objectives of this study are to establish a partitioning model between gaseous and particulate phases for PBDEs, which can reveal the real partitioning mechanism of PBDEs between these two phases and to predict the partition quotients defined in Eq. (1) accurately for PBDEs in air, thus to achieve a capability to address a series of G/P partitioning issues for these chemicals, such as those presented previously (Yang et al., 2013; Li and Jia, 2014).

2 Theory

2.1 Equilibrium state and steady state

To develop a new model in simulating G/P partitioning behavior, we need to understand the equilibrium state and steady state for SVOCs in environment. The steady state is a state in which no change occurs with time, or all time derivatives are equal to zero. "*Equilibrium* implies that phases have concentrations such that they experience no tendency for net transfer of mass" (Mackay 2001). These two terms have been frequently mistaken with each other. In his book (Mackay 2001), Mackay gave examples to explain the difference between these two states, indicating a chemical is in equilibrium between two media (phases) as long as its fugacities in the two media (phases) are equal no mater the system is steady or unsteady.

We also noticed that, although equilibrium is actually an ideal event since such a system cannot exist in real environment; this state has been successfully applied in some cases. Good examples are to treat air-water exchange for gaseous pesticide α-hexachlorocyclohexane (α-HCH) (Jantunen and Bidleman, 1996; 1997; Li et al. 2004) and air-soil exchange for gaseous polychlorinated biphenyls (PCBs) (Li et al. 2010). In these two examples, the factors other than the diffusion due to random molecular movement were negligible, and the systems can be treated as equilibrium, thus the net flux of gaseous α-HCH between air and water, and gaseous PCBs between air and soil are zero. We realized, however, that the exchange of SVOCs between the gas- and particle-phases is different since the advection processes, such as dry and wet depositions, caused by an external force (gravity) on the particles, cannot be ignored in studying the partitioning behavior of SVOCs between these two phases. Therefore, we suggest that the steady state, not equilibrium state, should be applied here.

2.2 G/P partitioning model under steady state

2.2.1 Basic equation

A model to describe G/P partitioning under steady state for PBDEs is

$$N_{\mathrm{G\text{-}P}} = N_{\mathrm{P\text{-}G}} + N_{\mathrm{P\text{-}S}} \tag{9}$$

where $N_{\mathrm{G\text{-}P}}$ is flux of PBDEs from gas phase to particle phase, $N_{\mathrm{P\text{-}G}}$ is flux of PBDEs from particle phase to gas phase, and $N_{\mathrm{P\text{-}S}}$ the net flux of particle-bound PBDEs between air and earth surface, such as water body or surface soil. For the sake of simplicity, we only consider dry and wet depositions in $N_{\mathrm{P\text{-}S}}$, which is given by (Mackay 2001)

$$N_{\mathrm{P\text{-}S}} = f_{\mathrm{P}}(D_{\mathrm{D}} + D_{\mathrm{W}}) \tag{10}$$

where f_{P} is fugacity of particle in air, given by Eq. (S1) in the Supplement with subscript “I” being “P”, and D_{D} is D value of dry deposition of particle-phase PBDEs described by (Mackay 2001)

$$D_{\mathrm{D}} = U_{\mathrm{D}} v_{\mathrm{P}} A Z_{\mathrm{P}} \tag{11}$$

where $\mathrm{U_D}$ is dry deposition velocity, a typical value being 10 m/h, A is the area between air and earth (water or soil), and Z_{P} is Z value of aerosol, given by Eq. (S3) in the Supplement, and v_{P} is the volume fraction of aerosol, given by

$$v_{\mathrm{P}} = 10^{-9} TSP/\rho \tag{12}$$

where TSP is the concentration of total suspended particles in air (μg m^{-3}) and ρ is the density of the particle (kg m^{-3}).

D_{W} is D value of wet deposition given by (Mackay 2001)

$$D_{\mathrm{W}} = U_{\mathrm{R}} Q v_{\mathrm{P}} A Z_{\mathrm{P}} \tag{13}$$

where U_{R} is rain rate, a typical value being 0.5 (m year^{-1}). Q is a scavenging ratio representing the volume of air efficiently scavenged by rain of its particle content, per unit volume of rain. A typical value for Q of 200,000 may be used. Substituting the above 2 Equations in Eq. (10) leads to

$$N_{P\text{-}S} = f_P\,(U_D+U_R Q)\,v_P A Z_P \tag{14}$$

2.2.2 Gas/particle exchange of PBDEs

One of the most important issues for investigating the G/P partitioning behavior is the exchange of PBDE between air and particle. We treat each particle as a ball with a mean diameter of d, a volume of $v=\pi d^3/6$, surface area $a=\pi d^2$, and a mass $m=\rho v$, where ρ is the density of the particle. The number of particles in 1 m^3 of air, $n = TSP/m$. In air with volume of Ah (h is the height of atmosphere), the total area of the particles is

$$A_P = 6TSP(\text{g m}^{-3})\times A(\text{m}^2)h(\text{m})/(\rho(\text{g m}^{-3})d(\text{m})) \tag{15}$$

Assuming $\rho = 1.5\times10^6$ g m^{-3}, $d = 1.0\times10^{-7}$ m (Rissler et al. 2006), $h = 1.0\times10^3$ m, the above equation becomes

$$A_P = 0.04A\times TSP \tag{16}$$

To be simplified, we treat the particles as a film, called the *particle film*, with a thickness of d, a surface area of A_P, as shown in **Fig. S1** in the Supplement. The ratio between A_P and A is

$$R_P = A_P / A = 0.04\ TSP \tag{17}$$

which is a linear function of TSP.

In order to study the movement of SVOCs between air and particle, we adapted the method used for the air-soil interface introduced by Mackay (2001). For diffusion, the two-resistance approach is used, and the overall D values is given by

$$1/D_V = 1/D_E + 1/(D_A + D_H) \tag{18}$$

where D_E is air boundary layer D value, D_A and D_H are diffusion D values of chemical in air and water sub-phases in particle film, respectively. D_E is deduced as the product of the surface area of the particle film, A_P (m^2), a mass transfer coefficient k_V (m h^{-1}), and the Z value of air Z_G, given by:

$$D_E = A_P\, k_V Z_G \tag{19}$$

Here,

$$k_V = B_a / l_a \tag{20}$$

where B_a is the chemical's molecular diffusivity in air (0.018 m^2 h^{-1} was assumed), and l_a is an air boundary layer thickness (0.00475 m was assumed) (Mackay 2001).

In comparison to the soil surface in air-soil exchange, the particle-film that we suggested in our model keeps moving within the atmosphere and thus has much more chances to intersect with the chemical in gas phase. Therefore, the mass transfer coefficient will be larger than that given by Eq. (20), and accordingly, a parameter C is introduced in Eq. (20), leading to

$$k_V = C B_a / l_a \tag{21}$$

Thus the term CB_a is the chemical's molecular diffusivity for the particle film in air, and its value will be determined later.

Since most of the SVOCs (including PBDEs) are associated with the organic matter of the particles, again for the sake of simplicity, the 2 terms, D_A and D_H, in Eq. (18) are neglected, which becomes

$$D_V = D_E = A_P k_V Z_G \tag{22}$$

The flux of PBDEs from gas phase to particle phase, $N_{G\text{-}P}$, becomes

$$N_{G\text{-}P} = f_G D_E \tag{23}$$

and the flux from particle phase to gas phase, $N_{P\text{-}G}$, is

$$N_{P\text{-}G} = f_P D_E \tag{24}$$

If the term $N_{P\text{-}S}$ is dropped from Eq. (9), i.e., the net flux of particle-bound PBDEs between air and surface is neglected, we will have

$$N_{G\text{-}P} = N_{P\text{-}G} \tag{25}$$

From Eqs. (23) and (24), the fugacities of a chemical in gas phase (f_G) and in particle phase (f_P) are equal, and thus the steady state becomes equilibrium. Therefore, it is concluded that equilibrium is just a special case of steady state when $\boldsymbol{N_{P\text{-}S}}$ is ignored.

2.3 G/P equations under steady state

2.3.1 G/P partition coefficient under steady state

We use Eqs. (10), (23), and (24) into Eq. (9), leading to

$$f_p(D_E + D_D + D_W) = f_G D_E \tag{26}$$

By using Eqs. (S6) and (S7) in the Supplement, the above equation leads to

$$C_p'/C_G = (Z_P/Z_G)(D_E / (D_E + D_D + D_W)) = K_{PG}\,(1 / [1 + (D_D + D_W) / D_E])$$

where C'_P (pg/m^3 of *particle*) and C_G (pg/m^3 of *air*) are concentrations of SVOCs in particle- and gas-phases, respectively, and K_{PG} is dimensionless *G/P partition coefficient* under equilibrium (= Z_P/Z_G). Setting a parameter α as

$$\alpha = 1 / [1 + (D_D + D_W) / D_E] \tag{27}$$

and the above equation becomes

$$C'_p/C_G = \alpha K_{PG} \qquad \text{(at } \textit{steady state}\text{)} \tag{28}$$

By using Eqs. (S10) and (S11), C'_p and K_{PG} are replaced by C_p and K_{PE}, respectively, Eq. (28) becomes

$$(C_P / TSP) / C_G = \alpha K_{PE} \tag{29}$$

Defining a *G/P partition coefficient under steady state*,

$$K_{PS} = (C_P / TSP) / C_G \qquad \textit{(at steady state)} \tag{30}$$

where C_G and C_P are concentrations of PBDEs in gas- and particle-phases (both in pg m^{-3} of air), respectively, *at steady state*, and the subscript "S" in K_{PS} indicates steady state. Although Eq. (30) seems the same as Eq. (1) (for K_P) and Eq. (S8) (for K_{PE}), they are different since Eq. (30) is defined under steady state, Eq. (S8) is under equilibrium, and Eq. (1) was defined at neither steady nor equilibrium state. Thus Eq. (29) becomes

$$\log K_{PS} = \log K_{PE} + \log\alpha \quad (31)$$

In the above equation, $\log K_{PE}$ is designated the *equilibrium term*, given by Eq. (3), and $\log\alpha$ is the *nonequilibrium term*. Therefore, we have two predicted partition coefficients: partition coefficient K_{PS} under steady state when the system is at steady state, or partition coefficient K_{PE} under equilibrium when the system is at equilibrium. Eq. (31) indicates that the equilibrium is just a special case of the steady state when $\log\alpha = 0$.

2.3.2 Nonequilibrium term $\log\alpha$

In Eq. (27), setting

$$G = C\,(D_D + D_W) / D_E \quad (32)$$

Eq. (27) becomes

$$\alpha = 1 / (1 + G/C) \quad (33a)$$

or

$$\log\alpha = -\log\,(1 + G/C) \quad (33b)$$

Substituting Eqs. (11), (13) and (19) in Eq. (32), which leads after some manipulations,

$$G = 2.09 \times 10^{-10} f_{OM} K_{OA} \quad (34)$$

Thus, as K_{PE} , $\log\alpha$ is also a function of f_{OM} and K_{OA}.

2.4 $\log\alpha$ as functions of $\log K_{OA}$ and temperature

Fig. S2 in the Supplement depicts variation of $\log\alpha$ as functions of $\log K_{OA}$ and temperature t with C=5. As shown in **Fig. S2A**, the function of $\log\alpha$ versus $\log K_{OA}$ is a curve shared by all PBDE congeners, showing that when $\log K_{OA} <$ ~10.4, $\log\alpha = 0$, the state is equilibrium. In contrast with the function of $\log\alpha$ versus $\log K_{OA}$, the functions of $\log\alpha$ versus t are different for different PBDE congeners, as shown in **Fig. S2B** in the Supplement. This figure explains why light PBDE congeners, such as BDE-17 and -28, can reach equilibrium state much more easily than heavy PBDE congeners. It is obvious from **Fig. S2B** that the curves of BDE-17 and -28 deviate significantly from zero at a low temperature (~ -10^{o}C), indicating that the values of logα are equal or close to 0 at a wide range of environmental temperature (t > -10^{o}C). For highly brominated congeners, BDE-153 for example, the values of logα deviates significantly from zero even when t < +40^{o}C, causing the equilibrium state at a much narrower ambient temperature range for this chemical (t > +40^{o}C) than BDE-17 and -28.

2.5 Threshold values of logK_{OA} and temperature

Since all the equations to calculate the parameter K_{PE} and K_{PS} link only the PBDE parameter logK_{OA}, it may be advantageous to explore partitioning behavior according to logK_{OA}, rather than individual PBDE congeners or homolog groups. Under this consideration, we drew logK_{PS} - logK_{OA} and logK_{PE} - logK_{OA} graphs, for all PBDE congeners/homologues at an environmental temperature range of -50 to +50 ^{o}C, as shown in **Fig. 1**. The straight line (thick blue) for logK_{PE} and the curve (red) for logK_{PS} can be used for all PBDE congeners/homologues as long as their ranges of logK_{OA} are known. Of course, it should be mentioned that the different PBDE congeners have different ranges of logK_{OA} at the same temperature span, thus are represented by different portions of the curves in the **Fig. 1**, accordingly showing different G/P partitioning behaviors.

There are three cases for G in Eq. (33b).

(1) G << C (D_D + D_W << D_E)

In this case, Eq. (33b) becomes

$$\log\alpha = -\log(1 + G/C) \approx 0 \qquad (35)$$

which is equilibrium state.

(2) G=C (D_D + D_W = D_E)

In this case, Eq. (33b) becomes

$$\log\alpha = -\log 2 \qquad (36)$$

If we assume that f_{OM} = 0.1 and C = 5, then we have the *first threshold value* from Eqs. (33b) and (34),

$$\log K_{OA1} = 11.4 \tag{37}$$

which is very close to the threshold value of $\log K_{OA}$ = 11.5 suggested by Li and Jia (2014). The physical meaning of $\log K_{OA1}$ is, at this threshold, the data of $\log K_{PS}$ deviates from $\log K_{PE}$ by an amount of log 2.

(3) G>>C ($D_D + D_W >> D_E$)

In this case, Eq. (33b) becomes

$$\log \alpha \approx -\log (G/C) = \log C - \log K_{PE} - 2.23 \tag{38}$$

thus $\log K_{PS}$ in Eq. (31) reaches its maximum value,

$$\log K_{PSM} = -1.53 \quad \text{or} \quad K_{PSM} = 0.03 \tag{39}$$

when $G>>C$. This is very close to the maximum value of -1.5 suggested by Li and Jia (2014). The maximum value of $\log K_{PS}$ is clearly shown in **Fig. 1** (the thin blue horizontal line), and we define the *second threshold value* as

$$\log K_{OA2} = 12.5 \tag{40}$$

As shown in **Fig. 1**, the first threshold value of $\log K_{OA}$ divides the whole range of $\log K_{OA}$ into *equilibrium* (EQ) and *nonequlibrium* (NE) *domains*. The second threshold indicates the start of the *maximum partition* (MP) *domain*, in which the values of $\log K_{PS}$ reach a maximum value of $\log K_{PSM}$, which is independent of the values of f_{OM} and K_{OA}.

In brief, as shown in **Fig. 1**, the curve of $\log K_{PS}$, originally coinciding with the straight line of $\log K_{PE}$, increases along with increase of $\log K_{OA}$, and separates visibly (by a mount of log2) from the straight line of $\log K_{PE}$ at the first threshold value of $\log K_{OA1}$, entering the NE domain from the EQ domain. After the second threshold value of $\log K_{OA2}$, the curve of $\log K_{PS}$ enters the MP domain and becomes a horizontal straight line of $\log K_{PS}$ = -1.53.

The values of $\log K_{OA}$ depend on each PBDE congener and the ambient temperature, as discussed previously (Harner and Shoeib, 2002). Accordingly, we defined two threshold values for temperature, the *threshold temperatures* t_{TH1} and t_{TH2}, which are the temperatures when $\log K_{OA}$ of PBDE congeners equals to the threshold values $\log K_{OA1}$ and $\log K_{OA2}$, respectively. As presented in **Fig. 2,** while the threshold values of $\log K_{OA1}$ and $\log K_{OA2}$ are constants for all congeners, the threshold values for t_{TH1} and t_{TH2} are different for different PBDE congeners. These two threshold temperature values divided the temperature space also into the same 3 domains; the EQ domain when $t > t_{TH1}$, the NE domain when $t \leq t_{TH1}$, and the MP domain when $t \leq t_{TH2}$. Taking BDE-47 as an example, with its $t_{TH1} = +11\,^{o}C$ and $t_{TH2} = -6\,^{o}C$, BDE-47 is in EQ domain when $t > +11^{o}C$; in NE domain when $t \leq +11^{o}C$; and in MP domain at $t \leq -6\,^{o}C$.

2.6 Particle phase fraction

Another important parameter, the fraction of chemical on the particle phase, ϕ (= $C_P/(C_G+C_P)$), can be calculated from K_P as

$$\phi_{PX} = K_{PX}\, TSP \,/\, (1+ K_{PX}\, TSP) \tag{41}$$

where the subscript "PX" can be one of "PS", "PE", and "PR" . Thus the maximum value of particle phase fraction can be obtained from Eqs. (39) and (41) as

$$\phi_{PSM} = 0.03\, TSP \,/\, (1+ 0.03\, TSP) \tag{42}$$

which indicates that, while the maximum partition coefficient $\log K_{PSM}$ is a constant for all PBDE congeners, it's corresponding maximum value of particle phase fraction is not, but depends on *TSP*. The variation of ϕ_{PSM} as a function of *TSP* is depicted in **Fig. S3** in the Supplement.

3. Application of the equations

3.1 G/P partitioning of PBDEs in Chinese Air from China-SAMP-II

In the previous section, we derived an Eq. (31) to predict the values of *partition coefficient under steady state* K_{PS}. In this subsection, we used these equations to predict K_P for air samples collected at 15 sites across China under our PBDE monitoring program, China-SAMP-II (Yang et al., 2013, Li and Jia, 2014), and the results will be compared with the predicted values of *partition coefficient under equilibrium state* K_{PE}, obtained using Eq. (3); and the values of *partition quotient*, K_{PR}, obtained using Eq. (2) with the help of K_{PM}, calculated from Eq. (1) using the monitoring data C_P and C_G. Among the three modeled values (K_{PS}, K_{PE}, and K_{PR}), K_{PR} values are the ones most close to the values of K_{PM} since $\log K_{PR}$ values are obtained directly from $\log K_{PM}$ by least squares regression against $\log K_{OA}$, and the accuracy of the equations of K_{PS} and K_{PE} depends on how their results close to those given by K_{PR}.

Figs. S4 and S5 in the Supplement depict the variations of $\log K_{PS}$, $\log K_{PE}$, and $\log K_{PR}$ as functions of $\log K_{OA}$ for the 15 sampling sites and 10 PBDE congeners, respectively, both showing the curve of $\log K_{PS}$ is closer to the regression line of $\log K_{PR}$ than $\log K_{PE}$. It is worthwhile to point out that, for the best match between the results of $\log K_{PS}$ and $\log K_{PR}$ for PBDEs, C = 5 was used in Eq. (5) to calculate $\log K_{PS}$ in air at all the sampling sites with an exception of the site of Waliguan, where C = 50 was used. The reason why much higher value of C was used at this site will be explained later. **Fig. S5** also shows that, from the light PBDE congeners to the heavy ones, the ranges of $\log K_{OA}$ for each PBDE congeners (at temperature range of -22 ^{o}C – +38 ^{o}C) move from left to right, from smaller than $\log K_{OA1}$ for BDE-17 to larger than $\log K_{OA1}$ for BDE-183, or the states that these congeners reside in change from EQ domain to the NE domain, and finally reach the MP domain.

The 10 regression lines ($\log K_{PR}$) for the 10 PBDE congeners shown in **Fig. S5** are all presented in **Fig. S6** in the Supplement along with the curves of $\log K_{PE}$ and $\log K_{PS}$, indicating evidently that these 10 lines of $\log K_{PR}$ change their slopes m_O along the curve of $\log K_{PS}$, not the straight line of $\log K_{PE}$, and accordingly, the curve of $\log K_{PS}$ matches the monitored G/P partitioning data very well for all the 10 PBDE congeners in Chinese air.

We understand that, modelers are most interested in K_P values as a function of temperature for each PBDE congener. **Fig. S7** in the Supplement presents variations of $\log K_{PS}$, $\log K_{PE}$, and $\log K_{PR}$ as functions of temperature for the 10 PBDE congeners, indicating that, the curve of $\log K_{PS}$ matches the line of $\log K_{PR}$ for each PBDE congener, the highly brominated congeners in particular, dramatically well. It is interesting to note that the two threshold temperatures, t_{TH1} and t_{TH2}, designed by two vertical dashed lines, increase from the less brominated to highly brominated PBDEs. For example, the value of t_{TH1} of BDE-17 equals to -16.5 ^{o}C, meaning that this compound is in the EQ domain in the most ambient temperature range of ≥-16.5 ^{o}C, while for BDE-183, t_{TH1}=36.5 ^{o}C and t_{TH2}=15 ^{o}C, meaning that this compound is in the EQ domain only when t>36.5 ^{o}C, in the NE domain when t≤36.5 ^{o}C, and in the MP domain when t≤15.0 ^{o}C. We also calculated the modeled values of $\log K_{PS}$ for 5 typical PBDE congeners as functions of temperature from -50 to +50 ^{o}C, and the results are given in **Fig. S8** in the Supplement, showing that, along with decrease of temperature, the values of $\log K_{PS}$ for PBDE congeners increase to a maximum partition value; the more highly brominated the congener is, the higher is its value of the first threshold temperature (t_{TH1}, data are not shown) and the second threshold temperature (t_{TH2}), and thus the higher temperatures at which the congener reaches the NE and MP domains.

As shown in **Fig. 1**, the partitioning behavior of PBDEs depends on ambient temperature of sampling events. There are three squares presented in **Fig. 1** indicating the three regions with different temperature ranges, 0 − +50 ^{o}C (the orange one), -30 − +30 ^{o}C (the green one), and -50 − 0 ^{o}C (the blue one). Here, we take the two sampling sites from China-SAMP-II

(Yang et al., 2013; Li and Jia, 2014), one is Harbin in the northeast of China, with a sampling temperature range of -22 – +28 ^{o}C, within the green square, and the other is Guangzhou in the south of China, with a range of +8 – +38 ^{o}C, within the orange square, as examples to show how the threshold values can be used in study the G/P partitioning behavior of PBDEs.

We determined the ranges of logK_{OA} for the 10 PBDEs at the site of Harbin (vertical bars) based on the ambient temperature range of -22 – +28 ^{o}C at the site, and the results are presented in **Fig. 3**. The two threshold values of logK_{OA}, logK_{OA1} and logK_{OA2} (the horizontal light blue dashed lines), divide the space of logK_{OA} (the left axis) into three domains, the EQ, the NE, and the MP domains, and accordingly, the 10 PBDEs in Harbin air can be segregated into 3 groups; BDE-17 and 28 (3-Br homologue) as equilibrium EQ-group, BDE-47 and 66 (4-Br homologue) as semiequilibrium SE-group, and others (>4-Br homologues) as nonequilibrium NE-group. The dominant portions of logK_{OA} for the EQ-group (purple lines) are under the line of logK_{OA1}, i.e., these congeners are mainly in the EQ domain, while the dominant or whole portions of the NE-group (blue lines) are above the line of log K_{OA1}, indicating that these congeners are in the NE and the MP domains. The SE-group (green lines) is in both the EQ and the NE domains. It is noteworthy that, the major portions of log K_{OA} for the PBDE congeners in the NE-group were in the MP domain. These three domains can also be identified in the temperature space. In **Fig. 3**, the two threshold temperatures, t_{TH1} (the red diamonds) and t_{TH2} (the red square), are also shown (the right axis), which is similar to **Fig. 2**. In the real ambient temperature range, formed by the two red dashed lines (-22 ^{o}C and +28 ^{o}C) at the Harbin site, the major temperature portions of PBDEs in the EQ-group were in the EQ domain ($t<t_{TH1}$), those of the NE-group in the NE and MP domains ($t \geq t_{TH1}$), and those of the SE-group in both the EQ and NE domains.

Fig. 4 presents the logK_P - logK_{OA} graph for the 10 PBDEs in Harbin, which is almost identical to the one contained in the green square of **Fig. 1**. The ranges of logK_{OA} for the three groups and their corresponding logK_P - logK_{OA} diagram are also shown. For example, the logK_P - logK_{OA} diagram for the EQ-group (3-Br homologue), bound by the 2 purple dashed lines, is mainly in the EQ domain, with a small portion in the NE domain; the logK_P - logK_{OA} diagram for the SE group (4-Br homologue), contained by 2 green dashed lines, is mainly in the NE domain, with a small portion in the MP domain; and the logK_P - logK_{OA} diagram for the NE-group (>4-Br homologue), formed by the 2 blue dashed lines, is mainly in the NE and MP domains.

Similar analysis was carried out for the 10 PBDEs at the site of Guangzhou at an ambient temperature range of +8 – +38 ^{o}C at the site (Yang et al., 2013), and the results are presented in **Figs. S9 and S10** in the Supplement. The 10 PBDEs at Guangzhou air can also be segregated into 3 groups, BDE-17, -28, and -47 as EQ-group, BDE-66, 99, and 100 as SE-group, and the others, BDE-85, -99, -100, and -183 as NE-group, which are quite different from those for Harbin, caused by the different ambient temperature ranges at the two sites.

We concluded that the PBDEs in Chinese air at 15 sampling sites across China were in the steady state instead of equilibrium state, in realizing that, for less brominated PBDE congeners, BDE-17 and -28, this steady state can be treated as equilibrium state since their nonequilibrium term (logα) can be ignored in comparison to the equilibrium term (logK_{PE}) in the temperature range of -22 ^{o}C to +38 ^{o}C (see **Fig. S2B**).

3.2 G/P partitioning of PBDEs in air from other sources

There are only a few data available in the literature that we can compare to our prediction data.

We predicted the partitioning behavior of gaseous and particle-bound PBDEs in the atmosphere at an e-waste site and a rural site in southern China during 2007-2008 using the information given by Tian et al. (2011). We calculated the values of logK_{PS}, logK_{PE}, and logK_{PR} as functions of logK_{OA}, and the results are presented in **Fig. S11.** It is noticeable that our predicted results are obviously better than those obtained by the equilibrium model at the rural site, but not at the e-waste site, where the data from equilibrium model matched the monitoring data better than those predicted using our equation. This seemed unexpected but could possibly be explained by the fact that the emissions of PBDEs from the e-waste site compensated the flux of PBDEs due to dry and wet deposition, leading a situation that seemed to be at equilibrium. We cannot, however, accept the point of view that the PBDEs in air at the rural area cannot reach equilibrium, but those in air at the e-waste sites can.

The G/P partitioning behavior was studied for 7 PBDEs (BDE-28, -47, -99, -100, -153, -154 and -209) at four sites (1 suburban, 2 urban, and 1 industrial) in Izmir, Turkey, in summer and winter in 2004-2005 with a temperature range of 1.8 – 22.4 ^{o}C (Cetin and Odabasi, 2007) . We calculated the particle phase PBDEs fractions ϕ_{PS} and ϕ_{PE}, using Eq. (41) and compared them with the monitoring data, and the results are depicted in **Fig. S12**. It was noted by the authors that their monitoring data were much lower than the predicted values by the equilibrium equation (ϕ_{PE}) (Cetin and Odabasi, 2007), but it is obvious that their results matched our predicted data (ϕ_{PS}) very well, among which, the best agreement was observed for BDE-209, the most highly brominated congener of PBDEs.

We calculated the G/P partition coefficients for PBDEs in atmosphere of Kyoto, Japan, which were measured in August 2000, and January and September 2001 (Hayakawa et al., 2004), and the variations of logK_{PE} and logK_{PS} as functions of logK_{OA} are presented in **Fig. S13,** indicating obviously that the values of logK_{PS} was in a better agreement with the monitoring data than logK_{PE}.

Air samples were collected from 1 urban, 2 rural, and 1 remote sites near the Great Lakes in 1997-1999 as part of the Integrated Atmospheric Deposition Network (IADN), among which, those taken when the ambient atmospheric temperatures were 20 ± 3 ℃ were analyzed for the G/P partitioning behavior of PBDEs, and the log-log relation of K_P and their subcooled liquid vapor pressures (P_L) for BDE-47, -99, -100, -153, and -154 were calculated (Strandberg et al. 2001). By using these data, we calculated both logK_P and ϕ_P as functions of logK_{OA} for the same 5 PBDE congeners, using the values of f_{OM} = 0.2 and TSP = 25 μg m^{-3} suggested by Harner and Shoeib (2002), which are presented in **Fig. S14**, along with the predicted results under equilibrium state and steady state. Again the results indicated that the prediction by our new equation is more accurate than those by the equilibrium equation.

3.3 G/P partitioning of PBDEs in the Arctic air

As discussed in the previous sections, each PBDE congener will reach the maximum partition domain when logK_{OA} ≥ logK_{OA2} or $t \leq t_{TH2}$. The value of t_{TH2} of BDE-183 is 15 °C, meaning that BDE-183 in air will be in MP domain when t < 15 °C. The value of t_{TH2} for BDE-209 should be higher (logK_{OA}=14.98 for BDE-209 was estimated at 25 °C by Cetin and Odabasi (2007) in comparison to logK_{OA}=11.97 for BDE-183 at the same temperature). Accordingly, BDE-209 in arctic air should be in the MP domain, with a constant of logK_{PSM} (= -1.53) and the corresponding ϕ_{PSM} (=0.23 if TSP = 10 μg m^{-3} is assumed). This prediction was remarkably in agreement with monitoring data for BDE-209 measured in arctic air at Alert, Canada from 2007 to 2009 with a temperature range between 10 and -50 °C (NCP 2013), lower than the value of t_{TH2} for BDE-209 (see **Fig. 5**). The comparisons between the predicted values and the monitoring data at Alert for other values of TSP (= 5 and 2 μg m^{-3}) given in **Fig. S15** also showed great consistence. It should be stressed from the figure that the values of logK_{PE} of BDE-209 are from 3.06 at 10 °C to 8.36 at -50 °C calculated by Eq. (3), which means that the values of K_{PE} are from more than 5 orders at 10 °C to 10 orders at -50 °C of magnitude higher than the monitoring data, a huge error that cannot be tolerated. The corresponding values of ϕ_{PE} are 1, indicating that BDE-209 are all in particle phase in the

Arctic air predicted by the equilibrium equation, which was not the case given by the monitoring data. In other words, the maximum value 0.23 of ϕ_{PSM} indicates that, from our prediction, more than half BDE-209 (~0.77) is in gas phase in arctic air, which was confirmed by the monitoring data shown in **Fig. 5**.

We also studied the G/P partition for the 10 PBDEs (BDE-28, -47, -66, -85, -99, -100, -153, -154, -183, and -209) in the Arctic atmosphere in East Greenland Sea in August and September 2009 with a temperature range between -0.5 ^{o}C and +6.5 ^{o}C (Möller et al., 2011). We calculated the values of logK_{PS}, logK_{PE}, and logK_{PR} as functions of logK_{OA}, and the results are shown in **Fig. S16**. Once again, the equation of logK_{PS} had a better performance than the equation of logK_{PE}, especially for those congeners in the NE domain with log$K_{OA} \geq$ logK_{OA1}.

4. Conclusions and Discussions

4.1 G/P partitioning of PBDEs in global air

Figure At a Glance in the Supplement presents G/P partition coefficients of PBDEs (logK_{PS} and logK_{PE}) as functions of logK_{OA} at ambient temperature ranging from -50 to +50 ^{o}C, which can be applied at any sites worldwide (the top middle panel, similar to **Fig. 1**). The three squares in the panel designate the logK_{P}-logK_{OA} graphs with three different temperature ranges: 0 − +50 ^{o}C, -30 − +30 ^{o}C, and -50 − 0 ^{o}C, representing the tropical and subtropical climate zones, warm temperate climate zone, and boreal and tundra climate zones, respectively. Monitoring data (logK_{PM}), their regression data (logK_{PR}), and the predicted results logK_{PS} and logK_{PE} in the three different temperature zones are presented in the figure; the site Guangzhou, China, within the subtropical climate zone, shown in the top-left panel, the site Harbin, China, within the warm temperate climate zone, shown in the bottom panel, and in the site Alert, Canada, within tundra climate zone, shown in the top-right panel, all introduced in the previous sections. The data at these three sampling sites all indicated that the curve of our new equation ($\log K_{PS}$) are superior to the equilibrium equation ($\log K_{PE}$) in G/P prediction of partitioning behavior for PBDEs in global air, at the sites in warm temperate, boreal, and tundra climate zones.

4.2 Equilibrium state vs steady state

Harner and Bidleman (1998) developed in 1998 the Eq. (3), which can predict for the first time the partition coefficients of selected SVOCs in air under the condition of equilibrium between gas- and particle-phases. Four years later, Harner and Shoeib (2002) used this equation to predict the partitioning behavior for 11 PBDE congeners at 25 ^{o}C and 0 ^{o}C, the results of which, along with the results from our new equation under steady state, are given in **Fig. S17** in the Supplement**.** As shown in the figure, the equilibrium Eq. (3) predicted that, at 0 ^{o}C, the particle fraction of PBDE congeners can reach as high as ~1, which means that PBDE congeners can completely sorbed to the particles. According to our new Eq. (31) under steady state, however, the maximum particle fraction of PBDE congeners was about 0.42 when $\log K_{OA} \geq \log K_{OA2}$, which was less than half of the highest values predicted by Eq. (3). In other words, we predict that the maximum particle fraction of PBDE congeners in air cannot be more than 50% under steady state if *TSP* < 30 μg/m^3 (See **Fig. S3** in the Supplement). In order to support their prediction results, Harner and Shoeib (2002) used the monitoring data of gaseous and particle-bound PBDEs in the Great Lakes air at 20±3 ℃ (Strandberg et al. 2001). However, as demonstrated in **Fig. S14**, the prediction by our new equation is much accurate than those by the equilibrium equation. This suggests that PBDEs in the Great Lakes atmosphere were in the steady state, not in the equilibrium state.

In brief, we cannot treat the gas- and particle-phases as a closed system for studying G/P partitioning behavior of PBDEs, since the third compartment, the surface of the earth has to be considered. If the nonequilibrium term, $\log\alpha$, in Eq. (31) cannot be ignored, then the fugacities of PBDEs in gas- and particle-phases are not equal, indicating that the system is not at equilibrium but at steady state. For some less brominated PBDEs (such as BDE-17 and -28) at certain temperature, the values of logα is small enough in comparison to the value of logK_{PE} in Eq. (31), which is considered as a small perturbation, the system can be considered as equilibrium.

4.3 The maximum partition coefficient

In our previous study (Li and Jia, 2014), we predicted for the first time by an empirical approach the existence of a maximum partition coefficient that every PBDE congener can reach, and was wrongly termed as "saturation state". This prediction was confirmed in this study by a theoretical approach. As shown in **Fig. 1**, the logarithm of the maximum partition coefficient logK_{PSM} is equal to -1.53 (or K_{PSM} = 0.03) when logK_{OA} ≥ logK_{OA2} (=12.5 for all PBDE congeners), or equally when the ambient temperature is smaller than or equal to t_{TH2}, which is from -34.5 ^oC for BDE-17 to 15 ^oC for BDE-183, and cannot increase linearly along with increase of logK_{OA} as predicted by the straight line of logK_{PE}. The difference of prediction data between these two equations can be very great. For example, as shown in **Fig. 1**, the difference can reach as high as ~5.5 order of magnitude when logK_{OA} = 17. Obviously, the state in the MP domain is a steady state, but not an equilibrium state since the fugacities of PBDEs in gas- and particle-phases are not equal.

The best example is the case for BDE-209 in the Canadian Arctic site Alert predicted by our new steady equation discussed previously (**Fig. 5**). In fact, this is true for any PBDE congener, not for BDE-209 only. As shown in **Fig. 1**, the blue square with a temperature range of -50 − 0 ^oC could most likely be the situation for the Arctic atmosphere. **Fig. 2** shows that, for the 7 PBDE congeners (BDE-66, -85, -99, -100, 153, -154, and -183), $t_{TH2} > 0$ ^oC. Thus we predict that, as the G/P partitioning behavior is considered, these 7 PBDE congeners do not behave differently in the Arctic air, and are all have the same partition coefficient,

$\log K_{PSM}$ = -1.53. Unfortunately, there are no data for the PBDE congeners other than BDE-209 available for confirmation of this prediction in the Arctic air.

4.4 Comparison to the empirical equations

The two empirical Eqs. (6) and (8) have been successfully applied to predict the values of K_P for PBDEs in air of China and other countries in the north temperate zone and also at an Arctic site in East Greenland (Li and Jia, 2014). The Eq. (31) for $\log K_{PS}$ derived in this study is superior to these empirical equations $\log K_{PP}$ and $\log K_{PP}$ (K_{OA}) in two ways. First, the steady-state Eq. (31) was derived theoretically, and secondly, this steady-state equation can be used at any ambient temperature, from equator to polar regions, while the empirical equations can only be used at a temperature range of -22 ^{o}C to +38 ^{o}C.

Comparison between steady-state Eq. (31) for $\log K_{PS}$ and empirical equations $\log K_{PP}$ given by Eq. (6) and $\log K_{PP}$ (K_{OA}) given by Eq. (8) in Harbin air at a temperature range of -22 to +28 ^{o}C are presented in **Fig. 6**, and the equilibrium equation $\log K_{PE}$, given by Eq. (3), is also included for comparison. It is evident from **Fig. 6** that, the straight line $\log K_{PP}$ deviates apparently from the straight line $\log K_{PE}$ at $\log K_{OA} = \log K_{OA1}$, and increases linearly with $\log K_{OA}$. Different lines of $\log K_{PP}$ (K_{OA}) for different PBDE congeners are able to predict the G/P partitioning behavior of PBDE more accurately than the straight line $\log K_{PP}$. It is interesting to note that, the different lines of $\log K_{PP}$ (K_{OA}) for different PBDE congeners change their trends along with the single line of steady-state equation $\log K_{PS}$, which is the best equation that can be used to predict the G/P partitioning behavior for all PBDE congeners and at all ranges of ambient temperature.

4.5 The limitation of applications

In order to derive Eq. (31), several assumptions were made, which include that, the G/P partitioning reached steady state, the annual rainfall was 0.5 m yr^{-1}, f_{OM} = 0.1, C = 5, and some others. This equation, however, has been successfully applied in all situations that we discussed in this study, in which some of the assumptions were not satisfied. We should be aware, however, that the situations in which some abnormal conditions exist, such as heavy wind, heavy rains, or the sampling sites close to e-waste or PBDE manufactures, should be best treated separately. For example, as described in the previous section, the constant *C* should be changed from 5 to 50 in Eq. (5) for Site Waliguan. The reason why much higher value of *C* was used at this site is possibly due to the high wind speed there. At Waliguan, where annual average wind speed reaches 4.6 m/s, and the northwest wind with speed > 10 m/s being quite often in the winter and spring seasons (http://gaw.empa.ch/gawsis/reports.asp?StationID=12), much higher than the other sites; and the air sampler was installed at the top of the mountain (see Supplementary Fig. S18), suffering from the highest wind speed without any blocks in the area, causing the higher value of *C* than those at the other 14 sites. An analytic equation may exist to relate the parameter *C* and the wind speed (and possibly other factors too), but this equation is not available at present and planned for future study. The case for the Chinese e-waste site is also worth to mention. Our equation cannot be used at the e-waste sites and most likely at the PBDE manufacturers as well since the emissions of PBDEs at these sites could be too large and also variable with time so that the steady state cannot be reached or maintained

It should be borne in mind that the steady state discussed here is still an idealized scenario since only dry and wet depositions were discussed in the study, other factors, such as humidity and artifacts, will also play roles to a certain extent to affect the G/P partitioning. As anticipated, results obtained from this study do not perfectly fit monitoring data. However, this study revealed the major internal factors governing the gas-particle partitioning processes for PBDEs, and explicated how these processes can be more correctly treated as being in steady state rather than in equilibrium state. At least, the steady-state model, not the equilibrium-state model, should be applied to analyze the gas-particle relationship of SVOCs, such as PBDEs. Further study for other SVOCs, like PCBs and PAHs, is on the way.

The Supplement related to this article is available online at

Author contribution:

Y.F.L. designed the research on the new theory of G/P partitioning of PBDE in air under steady state; Y.F.L., W.L.M., and M.Y. performed the research; Y.F.L., W.L.M, and M.Y. analyzed data; and Y.F.L. wrote the paper, with input from W.L.M., and M.Y.

Acknowledgment

This work was supported by the Fundamental Research Funds for the Central Universities (Grant No. HIT.KISTP.201427) and the National Natural Science Foundation of China (No. 21277038). The authors thank IJRC-PTS colleagues and students for their contributions to the China POPs SAMP-II. Valuable comments and editorial work from K. Kannan from Wadsworth Center, New York State Department of Health, and Department of Environmental Health Sciences, School of Public Health, State University of New York at Albany, J. Li from Stanford University, M. Alaee from Environment Canada, and Y. Su from Ontario Ministry of Environment, Canada, are highly appreciated. Thanks are also to D. Mackay of Trent University, Canada, for his encouragement and valuable comments when Y.F. Li (one of the coauthors) presented this work to Mackay's group.

References

Barrie, L. A., Gregor, D., Hargrave, B., Lake, R., Muir, D., Shearer, R., Tracey, B., and Bidleman, T.: Arctic contaminants: sources, occurrence and pathways. Sci. Total Environ., 122, 1-74, 1992.

Bidleman, T. F.: Atmospheric processes. Environ. Sci. Technol., 22, 361-367, 1988.

Bidleman, T. F. and Harner, T.: Sorption to Aerosols, in Handbook of Property Estimation Methods for Chemicals: Environmental and Health Sciences. (eds Boethling, R,S. and Mackay, D.), Lewis Publishers, Boca Raton, FL. 2000.

Bidleman, T. F., and Foreman, W. T.: 1987. Vapor-particle partitioning of semivolatile organic compounds. In Sources and Fates of Aquatic Pollutants, ed. R. A. Hites and S. J. Eisenreich, pp. 29-56. American Chemical Sot., Washington, District of Columbia.

Cetin, B. and Odabasi, M.: Atmospheric concentrations and phase partitioning of polybrominated diphenyl ethers (PBDEs) in Izmir, Turkey. Chemosphere 71, 1067-1078, 2007.

Eckhardt, S. K. B. and Manø, S. S. A.: Record high peaks in PCB concentrations in the Arctic atmosphere due to long-range transport of biomass burning emissions. Atmos. Chem. Phys., 7, 4527-4536, 2007.

Finizio, A., Mackay, D., Bidleman, T. F., Harner, T.: Octanol-air partition coefficient as a predictor of partitioning of semi-volatile organic chemicals to aerosols. Atmos. Environ., 15: 2289-2296, 1997.

Halsall, C. J. L., Barrie, A., Fellin, P., Muir, D.C.G., Billeck, B.N., Lockhart, L., Rovinsky, F. Ya., Kononov, E.Ya., and Pastukhov, B.: Spatial and temporal variation of polycyclic aromatic hydrocarbons in the Arctic atmosphere. Environ. Sci. Technol., 31, 3593-3599, 1997.

Harner, T. and Bidleman, T. F.: Octanol-air partition coefficient for describing particle/gas partitioning of aromatic compounds in urban air. Environ. Sci. Technol., 32, 1494-1502, 1998.

Harner, T. and Shoeib, M.: Measurements of octanol-air partition coefficients (K_{OA}) for polybrominated diphenyl ethers (PBDEs): Predicting partitioning in the environment. J. Chem. Eng. Data, 47, 228-232, 2002.

Hayakawa K, Takatsuki H, Watanabe I, Sakai S.: Polybrominated diphenyl ethers (PBDEs), polybrominated dibenzo-p-dioxins/dibenzofurans (PBDD/Fs) and monobromo-polychlorinated dibenzo-p-dioxins/dibenzofurans (MoBPXDD/Fs) in the atmosphere and bulk deposition in Kyoto, Japan. Chemosphere, 57, 343-356, 2004.

Helm, P. A. and Bidleman, T. F.: Gas–particle partitioning of polychlorinated naphthalenes and non- and mono-ortho-substituted polychlorinated biphenyls in arctic air. Sci. Total. Environ., 342, 161-173, 2005.

Hung, H., Blanchard, P., Poole, G., Thibert, B., Chiu, C. H.: Measurement of particle-boundpolychlorinated dibenzo-p-dioxins and dibenzofurans (PCDD/Fs) in Arctic air at Alert, Nunavut, Canada. Atmos. Environ., 36, 1041-1050, 2002.

Jantunen, L. M. and Bidleman, T.: Air-water gas exchange of hexachlorocyclohexanes (HCHs) and the enantiomers of α-HCH in Arctic regions. J. Geophys. Res., 101, 28837-28846, 1996.

Jantunen, L. M. and Bidleman, T.: Correction to “Air-water gas exchange of hexachlorocyclohexanes (HCHs) and the enantiomers of α-HCH in arctic regions” by Liisa M Jantunen and Terry Bidleman. J. Geophys. Res., 102, 19279-19282, 1997.

Li Y. F. and Jia, H. L.: Prediction of Gas/Particle Partition Quotients of Polybrominated Diphenyl Ethers (PBDEs) in north temperate zone air: An empirical approach, Ecotoxic. Environ. Safety, 108, 65-71, 2014.

Li, Y. F., Bidleman, T. F., Barrie, L. A., and McConnell, L. L.: Global hexachlorocyclohexane use trends and their impact on the arctic atmospheric environment. Geophys. Res. Lett., 25, 39-41, 1998.

Li, Y. F. and Bidleman. T. F.: Correlation between global emissions of α-hexachlorocyclohexane and its concentrations in the Arctic Air. J. Environ. Inform., 1, 52-57, 2003.

Li, Y. F., Macdonald, R. W., Ma, J., Hung, H., Venkatesh, S., α-HCH Budget in the Arctic Ocean: The Arctic Mass Balance Box Model (AMBBM), Sci. Total. Environ., 324, 115-139, 2004.

Li, Y. F., Harner, T., Liu, L., Zhang, Z., Ren, N. Q., Jia, H., Ma, J., Sverko, E.: Polychlorinated biphenyls in global air and surface soil: Distributions, air - soil exchange, and fractionation effect. Environ. Sci. Technol., 44, 2784-2790, 2010.

Lohmann, R., Harner, T., Thomas, G. O. and Jones, K.C.: A comparative study of the gas–particle partitioning of PCDD/Fs, PCBs and PAHs. Sci. Total. Environ., 34, 4943-4951, 2000.

Macdonald, R. W., Barrie, L. A., Bidleman, T. F., Diamond, M. L., Gregor, D. J., Semkin, R. G., Strachan, W. M., Li, Y. F., Wania, F., Alaee, M., Alexeeva, L. B., Backus, S. M., Bailey, R., Bewers, J. M., Gobeil, C., Halsall, C. J., Harner, T, Hoff, J. T., Jantunen, L. M., Lockhart, W. L., Mackay, D., Muir, D. C., Pudykiewicz, J., Reimer, K. J., Smith, J. N., Stern, G. A..: Contaminants in the Canadian Arctic: 5 years of progress in understanding sources, occurrence and pathways. Sci. Total. Environ., 254, 93-234, 2000.

Mackay, D. 2001. Multimedia Environmental Models: The Fugacity Approach, 2nd Edition, Taylor & Francis, New York. p: 261.

Möller, A, Xie, Z, Sturm R, and Ebinghaus, R.: Polybrominated diphenyl ethers (PBDEs) and alternative brominated flame retardants in air and seawater of the European Arctic. Environ. Pollut., 159, 1577-1583, 2011.

NCP 2013: Canadian Arctic Contaminants Assessment Report On Persistent Organic Pollutants – 2013 (eds Muir D, Kurt-Karakus P, Stow J.). (Northern Contaminants Program, Aboriginal Affairs and Northern Development Canada, Ottawa ON. xxiii + 487 pp + Annex 2013.

Pankow, J. F.: An absorption model of gas/particle partitioning in the atmosphere. Atmos. Environ., 28, 185-188, 1994.

Pankow, J. F.: Interdependence of the slopes and intercepts from log-log correlations of measured gas-particle partitioning and vapor pressure—I. theory and analysis of available data. Atmos. Environ., 26A, 1071-1080, 1992.

Pankow, J.F.: Review and comparative analysis of the theories on partitioning between the gas and aerosol particulate phases in the atmosphere. Atmos. Environ., 21, 2275-2283, 1987.

Pankow, J.F.: Further discussion of the octanol/air partition coefficient Koa as a correlating parameter for gas/particle partitioning coefficients. Atmos. Environ. 32, 1493-1497, 1998.

Pankow, J. F., and Bidleman, T. F.: Effects of temperature, TSP and percent non-exchangeable material in determining the gas-particle partitioning of organic compounds. Atmos. Environ., 25A, 2241-2249, 1991.

Pankow, J. F., and Bidleman, T. F.: Interdependence of the slopes and intercepts from log-log correlations of measured gas-particle partitioning and vapor pressure-I. Theory and analysis of available data. Atmos. Environ., 26A, 1071-1080,1992.

Rissler, J., Vestin, A., Swietlicki, E., Fisch, G., Zhou, J., Artaxo, P., and Andreae, M.O.: Size distribution and hygroscopic properties of aerosol particles from dry-season biomass burning in Amazonia. Atmos. Chem. Phys., 6, 471-491, 2006.

Strandberg, B., Dodder, N. G., Basu, I., and Hites, R. A.: Concentrations and spatial variations of polybrominated diphenyl ethers and other organohalogen compounds in

Great Lakes air. Environ. Sci. Technol., 35, 1078-1083, 2001.

Su, Y., Lei, Y. D., Wania, F., Shoeib, M., Harner, T.: Regressing gas/particle partitioning data for polycyclic aromatic hydrocarbons. Environ. Sci. Technol., 40, 3558-3564, 2006.

Tian, M., Chen, S., Wang, J., Zheng, X., Luo, X., and Mai, B.: Brominated flame retardants in the atmosphere of e-waste and rural sites in Southern China: Seasonal variation, temperature dependence, and gas-particle partitioning. Environ. Sci. Technol., 45, 8819-8825, 2011.

Weschler, C. J. and Nazaroff, W.W.: Semivolatile organic compounds in indoor environments. Atmos. Environ., 42, 9018-9040, 2008.

Weschler, C. J.: Indoor/outdoor connections exemplified by processes that depend on an organic compound's saturation vapor pressure. Atmos. Environ., 37, 5455-5465, 2003.

Yamasakl, H., Kuwata, K., and Mlyamoto, H.: Effects of ambient temperature on aspects of airborne polycyclic aromatic. Environ. Sci. Technol., 16, 189-194, 1982.

Yang, M., Qi, H., Jia, H., Ren, N., Ding, Y., Ma, W., Liu, L., Hung, H., Sverko, E., and Li, Y. F.: Polybrominated diphenyl ethers (PBDEs) in air across China: Levels, compositions, and gas-particle partitioning. Environ. Sci. Technol., 47, 8978-8984, 2013.

Figure captions

Figure 1. Variation of logK_{PE} and logK_{PS} as functions of logK_{OA} with a temperature range of -50 − +50 ^{o}C. Two threshold values of logK_{OA} (logK_{OA1} and logK_{OA2}) are also shown, which divide the space of logK_{OA} into three domains: the equilibrium (EQ), the nonequilibrium (NE), and the maximum partition (MP) domains. The three squares designate the logK_P-logK_{OA} graphs with three different temperature ranges: 0 − +50 ^{o}C, -30 − +30 ^{o}C, an -50 − 0 ^{o}C, representing the tropical and subtropical climate zones, warm temperate climate zone, and boreal and tundra climate zones, respectively.

Figure 2. The first and second threshold temperatures, t_{TH1} and t_{TH2} for 10 PBDE congeners, which divide the temperature space into the same 3 domains (EQ, NE, and MP).

Figure 3. The range of logK_{OA} (the left axis) and the threshold temperatures (the right axis) for 10 PBDE congeners in Harbin air at a temperature range of -22 to +28 ^{o}C. The ranges of logK_{OA} for the 10 PBDE congeners are given by the vertical bars. The 2 horizontal light blue dashed lines give the 2 threshold values of logK_{OA1} and logK_{OA2}, and the red diamonds and red squares present respectively the two corresponding threshold temperatures, t_{TH1} and t_{TH2}. The former divides the space of logK_{OA} (the left axis) and the later divides the temperature space (the right axis) into three domains: the EQ domain, the NE domain, and the MP domain. Thus the PBDE congeners (homologues) in Harbin air can be segregated into 3 groups; BDE-17 and -28 (3-Br homologue) as equilibrium EQ-group, BDE-47 and -66 (4-Br homologue) as semiequilibrium SE-group, and others (>4-Br homologues) as nonequilibrium NE-group.

Figure 4. The logK_P - logK_{OA} diagram for the 10 PBDE congeners in Harbin air at a temperature range of -22 to +28 ^{o}C. The EQ Group includes BDE-17 and -28, the SE Group contains BDE-47 and -66, and the rests belong to NQ Group. The range of

$\log K_{OA}$ for each group and their corresponding $\log K_P$ - $\log K_{OA}$ diagram are also shown. The $\log K_P$ - $\log K_{OA}$ diagram for the EQ Group, boned by 2 purple dashed lines, is mainly in the EQ domain, with a small portion in NE domain; the $\log K_P$ - $\log K_{OA}$ diagram for the SE Group, contained by 2 green dashed lines, is mainly in the NE domain, with a small portion in MP domain; and the $\log K_P$ - $\log K_{OA}$ diagram for the NE Group, formed by the 2 blue dashed lines, is mainly in the NE and MP domains.

Figure 5. The temporal trends of concentrations of BDE-209 in the Arctic air in gas + particle phase (blue line) and in particle phase (green line) at Alert, Canada from 2007 to 2009 **(**NCP 2013**)**. The purple triangles and red diamonds are the values of ϕ and $\log K_P$ of BDE-209, respectively, calculated using the concentration data, and match well the values of ϕ_{PSM} (=0.23) and $\log K_{PSM}$ (-1.53), respectively (TSP = 10 μg m^{-3} was assumed).

Figure 6. Variation of $\log K_{PS}$ (the thick red line, given by Eq. (31)), $\log K_{PE}$ (the thick dark green line, given by Eq. (3)), and $\log K_{PP}$ (the thick pink line, given by Eq. (6)) as functions of $\log K_{OA}$. The functions of $\log K_{PP}(K_{OA})$ (the thin lines, given by Eq. (8)) vesus $\log K_{OA}$ for the 10 PBDE congeners in Harbin air at a temperature range of -22 to +28 ^{o}C are also included.

Figures

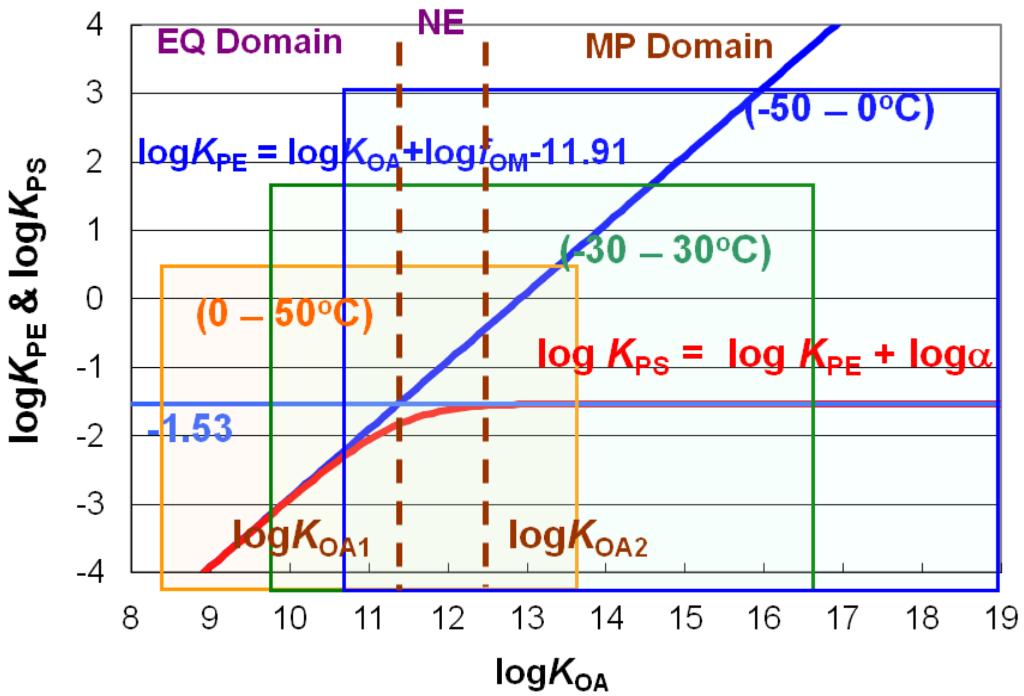

Figure 1. Variation of logK_{PE} and logK_{PS} as functions of logK_{OA} with a temperature range of -50 − +50 ^{o}C. Two threshold values of logK_{OA} (logK_{OA1} and logK_{OA2}) are also shown, which divide the space of logK_{OA} into three domains: the equilibrium (EQ), the nonequilibrium (NE), and the maximum partition (MP) domains. The three squares designate the logK_{P}-logK_{OA} graphs with three different temperature ranges: 0 − +50 ^{o}C, -30 − +30 ^{o}C, an -50 − 0 ^{o}C, representing the tropical and subtropical climate zones, warm temperate climate zone, and boreal and tundra climate zones, respectively.

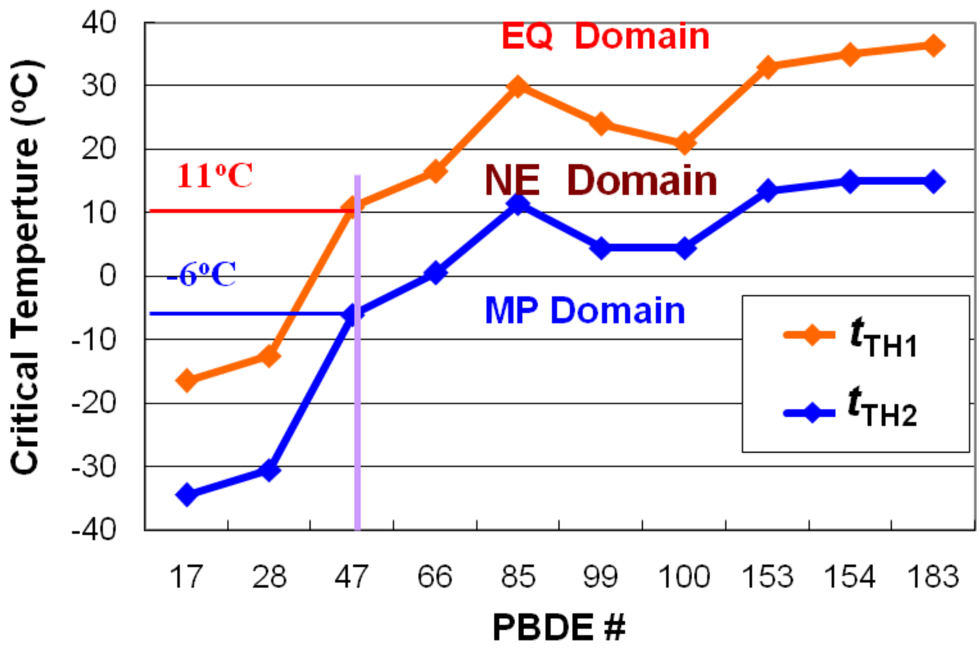

Figure 2. The first and second threshold temperatures, t_{TH1} and t_{TH2} for 10 PBDE congeners, which divide the temperature space into the same 3 domains (EQ, NE, and MP).

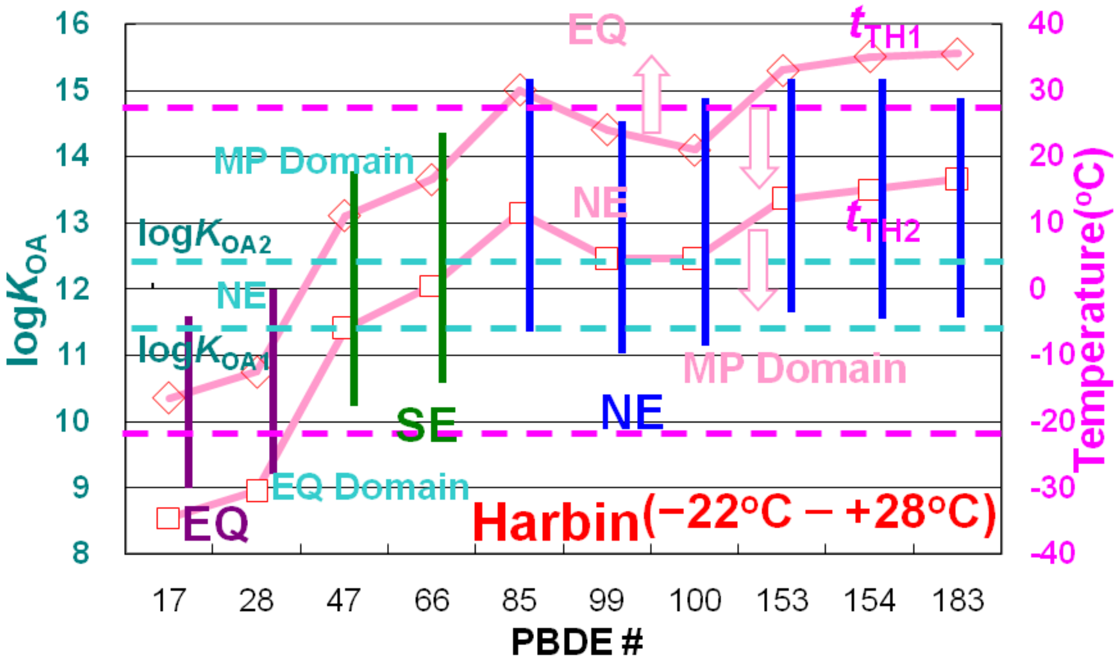

Figure 3. The range of logK_{OA} (the left axis) and the threshold temperatures (the right axis) for 10 PBDE congeners in Harbin air at a temperature range of -22 to +28 ^{o}C. The ranges of logK_{OA} for the 10 PBDE congeners are given by the vertical bars. The 2 horizontal light blue dashed lines give the 2 threshold values of logK_{OA1} and logK_{OA2}, and the red diamonds and red squares present respectively the two corresponding threshold temperatures, t_{TH1} and t_{TH2}. The former divides the space of logK_{OA} (the left axis) and the later divides the temperature space (the right axis) into three domains: the EQ domain, the NE domain, and the MP domain. Thus the PBDE congeners (homologues) in Harbin air can be segregated into 3 groups; BDE-17 and -28 (3-Br homologue) as equilibrium EQ-group, BDE-47 and -66 (4-Br homologue) as semiequilibrium SE-group, and others (>4-Br homologues) as nonequilibrium NE-group.

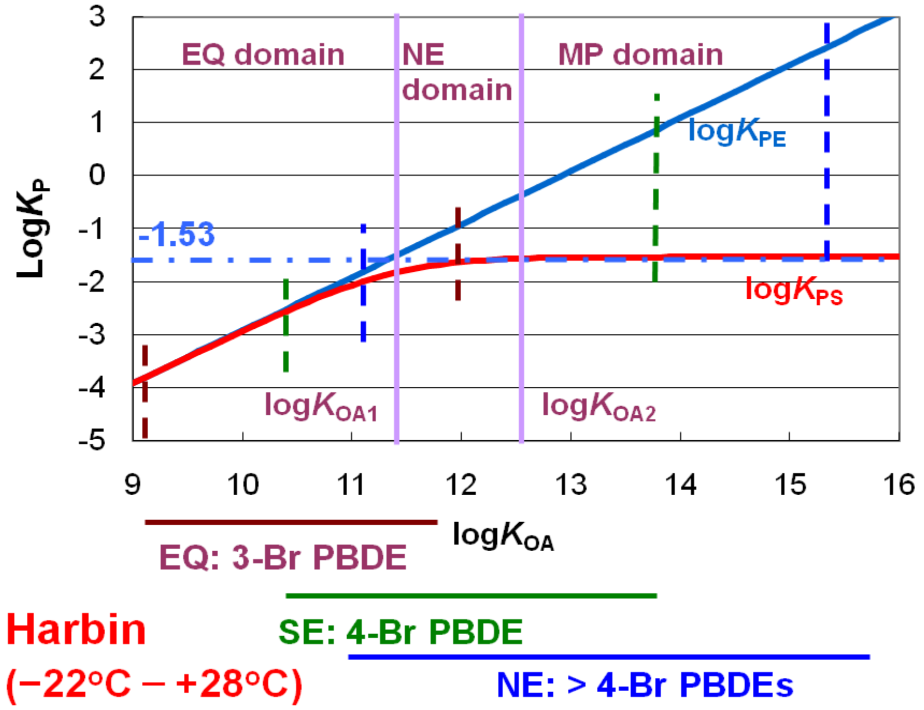

Figure 4. The logK_P - logK_{OA} diagram for the 10 PBDE congeners in Harbin air at a temperature range of -22 to +28 ^oC. The EQ Group includes BDE-17 and -28, the SE Group contains BDE-47 and -66, and the rests belong to NE Group. The range of logK_{OA} for each group and their corresponding logK_P - logK_{OA} diagram are also shown. The logK_P - logK_{OA} diagram for the EQ Group, boned by 2 purple dashed lines, is mainly in the EQ domain, with a small portion in NE domain; the logK_P - logK_{OA} diagram for the SE Group, contained by 2 green dashed lines, is mainly in the NE domain, with a small portion in MP domain; and the logK_P - logK_{OA} diagram for the NE Group, formed by the 2 blue dashed lines, is mainly in the NE and MP domains.

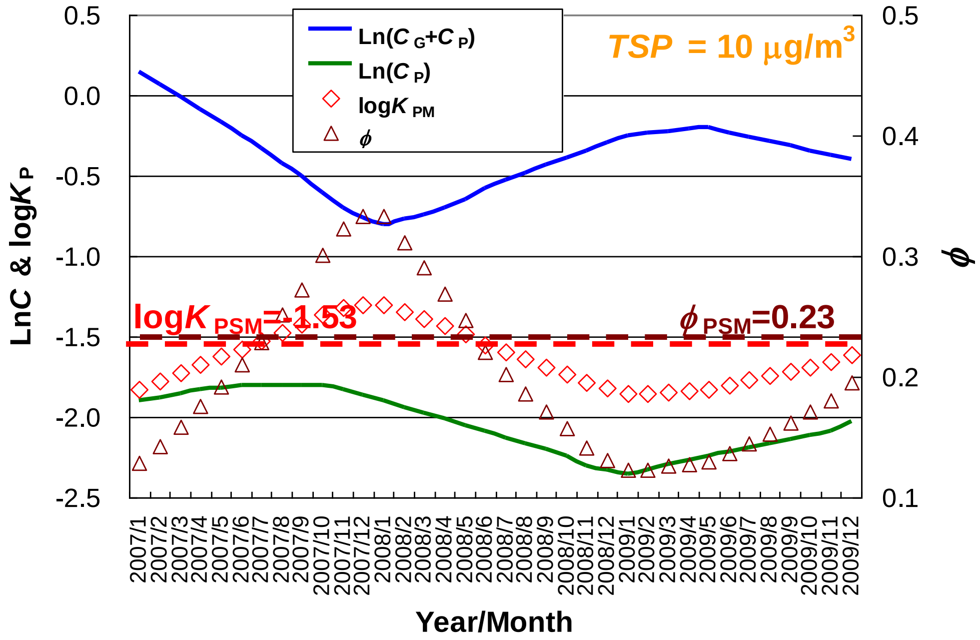

Figure 5. The temporal trends of concentrations of BDE-209 in the Arctic air in gas + particle phase (blue line) and in particle phase (green line) at Alert, Canada from 2007 to 2009 **(**NCP 2013**)**. The purple triangles and red diamonds are the values of ϕ and logK_{P} of BDE-209, respectively, calculated using the concentration data, and match well the values of ϕ_{PSM} (=0.23) and logK_{PSM} (-1.53), respectively (TSP = 10 μg m^{-3} was assumed).

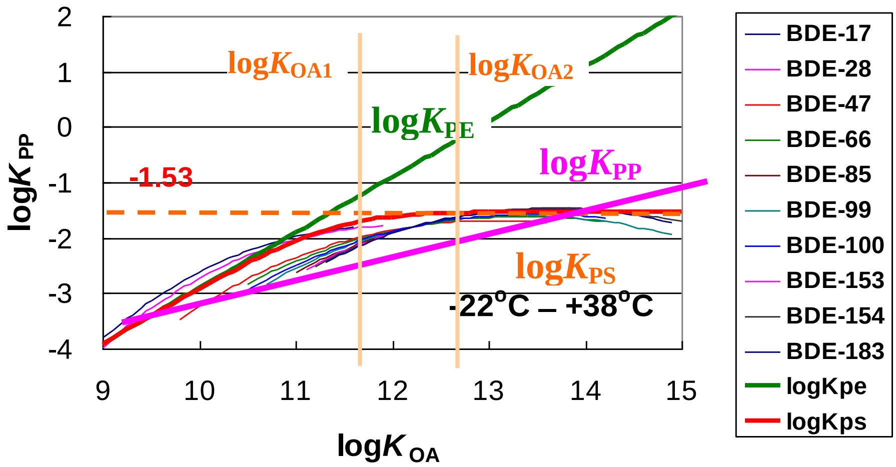

Figure 6. Variation of logK_{PS} (the thick red line, given by Eq. (31)), logK_{PE} (the thick dark green line, given by Eq. (3)), and logK_{PP} (the thick pink line, given by Eq. (6)) as functions of logK_{OA}. The functions of logK_{PP} (K_{OA}) (the thin lines, given by Eq. (8)) versus logK_{OA} for 10 PBDE congeners in Harbin air at a temperature range of -22 to +28 °C are also included.